Exchange bias in $LaFeO_3$ nanoparticles

2010 J. Phys. D: Appl. Phys. 43 245002

(http://iopscience.iop.org/0022-3727/43/24/245002)

IOP PUBLISHING JOURNAL OF PHYSICS D: APPLIED PHYSICS

J. Phys. D: Appl. Phys. **43** (2010) 245002 (5pp) doi:10.1088/0022-3727/43/24/245002

Exchange bias in $LaFeO_3$ nanoparticles

Hossein Ahmadvand[1], Hadi Salamati[1], Parviz Kameli[1], Asok Poddar[2], Mehmet Acet[3] and Khalil Zakeri[4]

[1] Department of Physics, Isfahan University of Technology, Isfahan 84156-83111, Iran
[2] Saha Institute of Nuclear Physics, 1/AF Bidhannagar, Kolkata 700064, India
[3] Fachbereich Physik, Experimentalphysik, Universität Duisburg-Essen, D-47048 Duisburg, Germany
[4] Max-Planck Institute of Microstructure Physics, Weinberg 2, D-06120 Halle, Germany

E-mail: ahmadvand@ph.iut.ac.ir

Received 19 February 2010, in final form 13 April 2010
Published 1 June 2010
Online at stacks.iop.org/JPhysD/43/245002

Abstract
Nanoparticles of antiferromagnetic $LaFeO_3$ were prepared by the sol–gel method. An exchange bias effect has been observed and is attributed to the exchange coupling between the ferromagnetic shell and antiferromagnetic core of the particles. The results provide clear evidence of the presence of spontaneous exchange bias in this system. After field cooling from room temperature, the exchange bias increases while the coercivity decreases with decreasing temperature. Taking into account the role of thermal activation, the temperature dependence of exchange bias and coercivity has been interpreted in terms of the spontaneous exchange bias mechanism proposed recently.

(Some figures in this article are in colour only in the electronic version)

1. Introduction

The subject of exchange bias (EB) has received considerable interest because of its important applications and fascinating fundamental physics [1]. An EB anisotropy appears in hybrid ferromagnetic–antiferromagnetic (FM/AFM) systems and manifests itself in the form of a shift of the hysteresis loop. Conventionally, the EB appears after cooling the system in the presence of a magnetic field through the Néel temperature (T_N) of AFM. However, a few reports have shown that the EB anisotropy is established even when the system is zero field cooled [2–4]. Recently, Saha and Victora [5], by micromagnetic simulation, proposed a mechanism for *spontaneous* EB in a bilayer system with a polycrystalline AFM. The term spontaneous refers to the case in which the system is not conventionally field cooled.

Extensive research has been done on the discovery of many different materials exhibiting EB properties. Most of these studies have been focused on bilayers, core–shell nanoparticles and FM nanoparticles embedded in an AFM matrix [1]. The presence of uncompensated surface spins also leads to an EB anisotropy in the nanostructures of AFM materials such as NiO [6], Co_3O_4 [7], CuO [8], Cr_2O_3 [9] and ferritin [10]. In particular, NiO has attracted much attention because of its relatively high T_N of 520 K. However, despite extensive research, the interesting magnetism of the AFM nanostructures has not been very well understood. Recently, the EB effect has been observed in perovskite oxides such as manganites [11, 12], cobaltites [13] and nanoparticles of AFM $BiFeO_3$ [14, 15]. Besides the EB effect, a weak ferromagnetism was also found in the nanoparticles of perovskite oxides such as $La_{1/3}Sr_{2/3}FeO_3$ [16] and $LaCoO_3$ [17].

Lanthanum orthoferrite ($LaFeO_3$) is a canted G-type AFM with a high $T_N = 750$ K [18] and has an orthorhombic distorted perovskite structure. In the perovskite structure, the Fe^{3+} ion is surrounded by six O^{2-} ions and forms an octahedron. Thin films of $LaFeO_3$ are excellent model systems for exploring the correlation between their crystalline, AFM domains and the resulting EB anisotropy when coupled to a FM layer, such as Co/$LaFeO_3$ [19]. In contrast, magnetic properties of $LaFeO_3$ nanopowders have been relatively less studied [20–22]. In this study, we report the first observation of EB properties in $LaFeO_3$ nanoparticles. We provide an interpretation of the temperature dependence of EB and coercivity, based on the spontaneous EB mechanism.

2. Experimental

Nanoparticles of $LaFeO_3$ were prepared using the sol–gel route. High purity $Fe(NO_3)_3 \cdot 9H_2O$, $La(NO_3)_3 \cdot 6H_2O$, citric acid ($C_6H_8O_7$) and ethylene glycol ($C_2H_6O_2$) were used as raw materials. Stoichiometric amounts of Fe and La nitrates

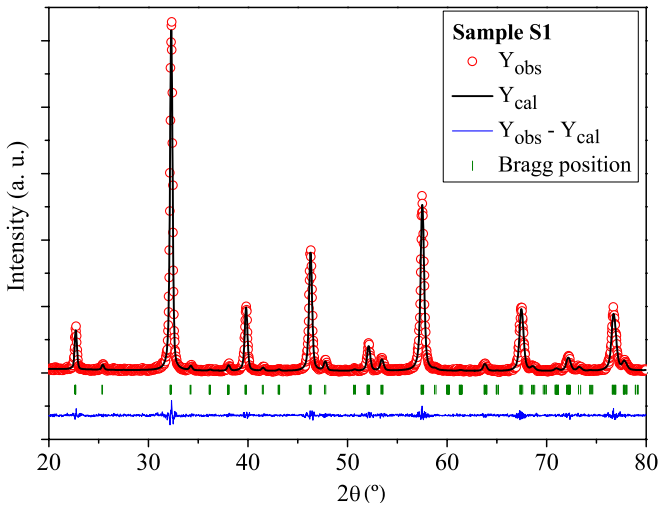

Figure 1. XRD pattern of sample S1. The circles are the experimental data (Y_{obs}), the solid line is the calculated pattern (Y_{cal}) and the bottom curve is the difference between the experimental and calculated patterns ($Y_{obs} - Y_{cal}$). The vertical bars are the Bragg reflections for the space group *Pnma*.

were mixed in deionized water and the obtained solution was dissolved in an aqueous solution of citric acid and ethylene glycol. The pH value of the solution was adjusted to 2–3 by adding ammonia solution. The obtained solution was dried at about 70 °C. The precursor powders were calcined at 600 °C (labelled S1) and 725 °C (labelled S2) for 5 h to obtain the nanocrystalline samples. The structural characterization of the samples was carried out using x-ray diffraction (XRD) with Cu $K\alpha$ radiation, field-emission scanning electron microscopy (FE-SEM) and transmission electron microscopy (TEM). The XRD patterns of the samples were analysed using the FULLPROF package [23]. Magnetization measurements were performed using a superconducting quantum interference device (SQUID) magnetometer.

3. Results and discussion

Figure 1 shows the experimental and calculated XRD patterns of sample S1. The analysis of the XRD patterns using the FULLPROF program shows that the samples have an orthorhombic crystal structure with the space group *Pnma*. No detectable secondary phase is observed in the patterns. The unit cell parameters were found to be $a = 5.561$ Å, $b = 7.848$ Å, $c = 5.552$ Å for sample S1 and $a = 5.561$ Å, $b = 7.843$ Å, $c = 5.552$ Å for sample S2. Figure 2 shows the typical FE-SEM images of the samples. The average particle size of sample S1 was estimated to be in the range 40–45 nm. For sample S2, by using FE-SEM and TEM (not shown here) images, the average particle size was estimated to be about 70 nm.

Figure 3 shows the temperature dependence of magnetization in the zero field cooling (ZFC) and field cooling (FC) processes under an applied field of 50 kOe between 5 and 340 K. As seen from figure 3 for both samples, the ZFC magnetization does not show a defined maximum. Moreover, there is a

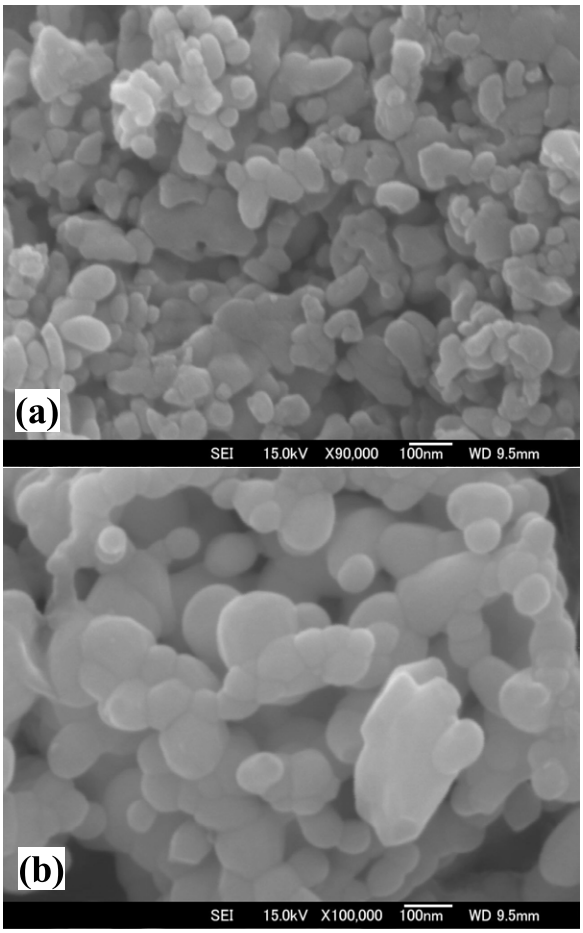

Figure 2. Typical FE-SEM images of sample S1 (*a*) and sample S2 (*b*).

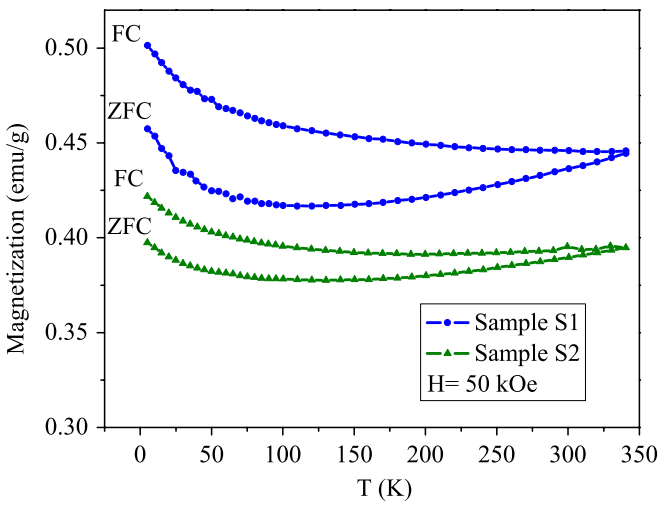

Figure 3. Temperature dependence of FC and ZFC magnetization of $LaFeO_3$ nanoparticles (samples S1 and S2) in an applied field of 50 kOe.

splitting between the ZFC and FC branches in the whole temperature range up to 340 K. Such splitting between the ZFC and FC magnetization at high magnetic fields below the T_N was also observed in the nanowires of Co_3O_4 [24]. It is also seen that the splitting decreases with increasing particle size.

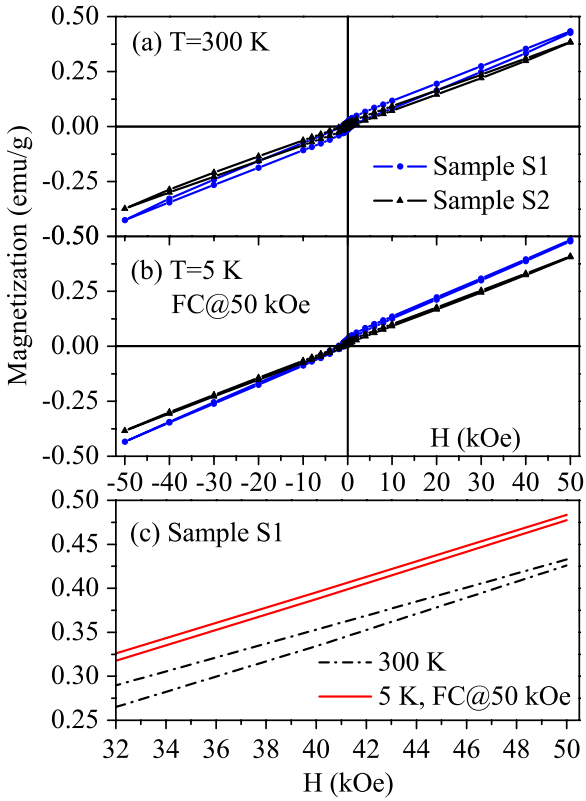

Figure 4. The M–H loops of $LaFeO_3$ nanoparticles (samples S1 and S2) at (*a*) 300 K, (*b*) 5 K after FC in 50 kOe and (*c*) shows the high-field region of the hysteresis loops for sample S1.

The relatively larger magnetization obtained for sample S1 can be attributed to the larger fraction of uncompensated surface spins which are responsible for *1/size* dependence of magnetization in the nanoparticles of AFM materials [6, 8, 15]. From figure 3, it can be understood that the T_N of the samples is higher than 340 K. Ita *et al* reported that while the bulk sample of $LaFeO_3$ has a T_N of 750 K, the nanoparticle sample with an average particle size of about 40 nm (similar to sample S1) has a lower T_N of 700 K [22].

The magnetic hysteresis loops measured at 300 and at 5 K after cooling the samples in a field of 50 kOe are shown in figure 4. For clarity, an enlarged view of the central part of the loops is also shown in figure 5. The observed linear M–H loop, as expected for a bulk AFM, indicates the presence of a predominant AFM phase. Moreover, a weak FM component is also clearly seen in the loops. This behaviour can be interpreted in terms of a core/shell model; the FM-like component comes from the surface of the particles and the field linear AFM contribution comes from the core spins [25]. The hysteresis loops remain open even in a high magnetic field of 50 kOe (figure 4(*c*)), as reported for other AFM nanoparticle systems [7, 8]. As seen from figures 5(*a*) and (*b*), the FC hysteresis loops for both samples show a shift H_E to the negative direction expected from the EB effect. Sample S1, which has a smaller particle size, shows a larger H_E at 5 K; $H_E^{S1} = 1550$ Oe, $H_E^{S2} = 1205$ Oe. This EB is attributed to the exchange coupling between the FM-like shell and AFM core of the particles. As discussed in [1], most of the studied exchange-biased nanoparticle systems are composed of FM

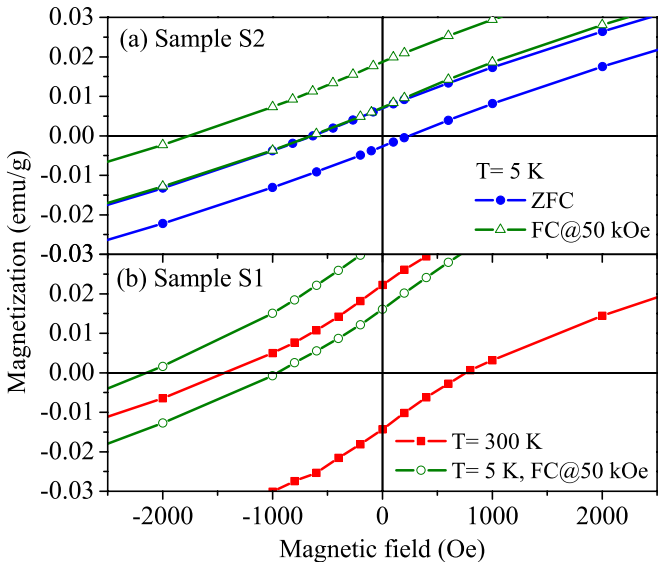

Figure 5. An enlarged part of the M–H loops of $LaFeO_3$ nanoparticles: (*a*) sample S2 at 5 K after ZFC and after FC in 50 kOe, (*b*) sample S1 at 300 K and 5 K after FC in 50 kOe.

cores and AFM shells. The FM(core)/AFM(shell) structure is inverted in the nanoparticles of AFM materials, i.e. a FM-like shell surrounds the AFM core. This situation is similar to the exchange-biased MnO/Mn_3O_4 system, where the AFM MnO is in the core [26, 27]. Alternatively, the EB anisotropy can be seen as an asymmetry in the remanence magnetization. The temperature dependence of the vertical magnetization shift (M_{EB}) follows a similar trend as the EB field (see the inset of figure 6). This shift is a manifestation of the presence of a unidirectional exchange anisotropy interaction and has also been observed in Co_3O_4 nanowires [7] and Pr-based manganites [11]. It is also seen that the appearance of the EB is accompanied by an enhancement of the coercivity ($H_C^{FC} > H_C^{ZFC}$) (figure 5(*a*)), characteristic of exchange-biased systems like CuO nanoparticles [8]. It should be mentioned that a nonzero shift to the negative direction is also observed at 300 and 5 K after ZFC. For sample S2, the coercivity and EB, after ZFC to 5 K, were found to be about 440 Oe and 200 Oe, respectively (figure 5(*a*)).

Besides the uncompensated surface spins, there are other factors which may contribute to the magnetization of $LaFeO_3$ nanoparticles. (i) The canted spin structure of $LaFeO_3$ gives rise to a weak ferromagnetism. Such behaviour may be enhanced at the surface of particles. (ii) Oxygen nonstoichiometry can change the valence state of Fe^{3+} and alter the magnetization. The formation of Fe^{2+} was reported to have a role in improving the magnetization of nanoscale $BiFeO_3$ [14]. (iii) Structural defects, broken exchange bonds and a smaller number of atomic neighbours induce a spin disorder at the surface of particles which may lead to a spin-glass-like behaviour [28, 29]. As discussed by Nogués *et al* [1], this spin-glass surface layer can act as FM on AFM nanoparticles. The observed open hysteresis loop at high magnetic fields (figure 4(*c*)) is a signature of the presence of a spin-glass phase at the surface of the particles [7, 30]. The opening of the hysteresis loop up to 50 kOe implies that some of the spin-glass-like surface spins presumably have a switching

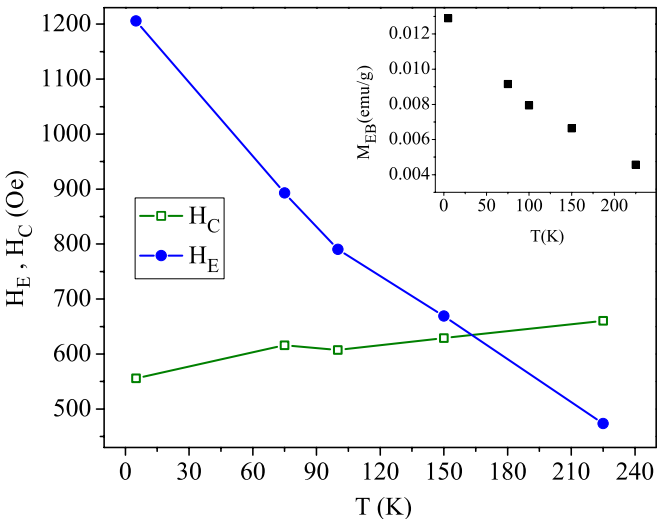

Figure 6. Temperature dependence of EB (H_E) and coercivity (H_C) for sample S2 after FC from room temperature in 50 kOe. Inset shows the temperature dependence of the vertical magnetization shift (M_{EB}).

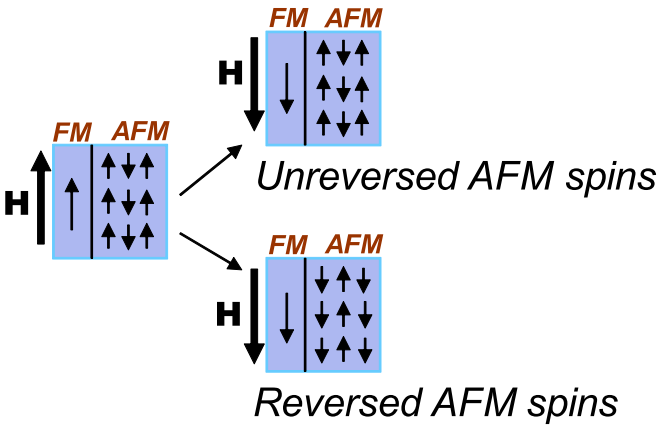

Figure 7. A schematic illustration of the possible orderings of the AFM (core) spins.

field higher than the applied field. The splitting between ZFC and FC magnetization (figure 3), which is characteristic of spin-glass-like behaviour [12, 30], gives further evidence for the existence of a surface spin-glass phase in $LaFeO_3$ nanoparticles. Due to the smaller surface/volume ratio for sample S2, the effect of surface disorder is smaller in this sample which manifests itself in the smaller splitting between ZFC and FC magnetization (figure 3).

Figure 6 shows the temperature dependence of EB and coercive fields of sample S2 after FC (50 kOe) from room temperature. Such a cooling process is not conventional FC, because the T_N of the prepared $LaFeO_3$ nanoparticles is much higher than room temperature. This means that the EB is established without the conventional FC of the system through the T_N. From figure 6 it is seen that the EB increases and coercivity decreases with decreasing temperature. A similar behaviour can be understood for sample S1 from figure 5(*b*), which shows that the coercivity at 5 K is smaller and the EB is higher than that at 300 K. In contrast to this behaviour, in the nanoparticles of $BiFeO_3$ [15] and other AFM materials [6, 8, 9], the increase in EB with decreasing temperature is usually accompanied by an increase in the coercivity. The temperature dependence of H_E and H_C can be interpreted using the spontaneous EB mechanism by considering the thermal activation of the AFM core of the particles. As reported by several groups [5, 31–33], thermally activated reversal of the AFM grains plays a crucial role in establishing EB anisotropy in nanostructures. The prepared $LaFeO_3$ nanoparticles represent a system of particles containing FM/AFM interfaces, with random anisotropies and with an energy barrier ($K_{AF} V_{AF}^{core}$) distribution, and hence show features similar to those previously used for simulation [5].

The application of the first field point (here 50 kOe) for loop evaluation spontaneously introduces a preferred direction in the system through some particles. When the direction of the field is reversed, larger particles do not have enough thermal energy to switch back. Such particles have fixed core spins, do not contribute to the hysteresis loop during the entire field cycle and induce a spontaneous EB anisotropy. In smaller particles, core spins follow the spins of the FM part during field reversal. In principle, one would expect that the particles with reversed AFM spins lead to an enhanced coercivity. Figure 7 simply shows the two possible orderings of the core (AFM) spins after reversing the magnetization of the FM part. The appearance of the EB at 300 and 5 K after ZFC is consistent with this interpretation. When the samples are field cooled from room temperature to lower temperatures, the thermal energy decreases and also the AFM anisotropy constant increases; thus more particles will be locked. Therefore, the number of particles with reversed core spins decreases with decreasing temperature, which leads to a lower H_C and a stronger H_E, as seen in figure 6. Finally, it is noteworthy that van Lierop *et al* [2] reported the observation of the EB effect in $Ni_{80}Fe_{20}/Co_3O_4$ thin films even when the system is zero field cooled. They argued that the temperature dependence of EB is dominated by thermal fluctuations.

4. Conclusion

In summary, we have shown that the nanoparticles of AFM $LaFeO_3$ exhibit EB properties. This effect originates from the coupling between the FM shell and the AFM core of the particles. Thermally activated reversal of the AFM spins can explain the appearance of EB without the conventional FC, as well as the temperature dependence of EB and coercivity.

Acknowledgments

This work was supported by Isfahan University of Technology (IUT). The authors thank Ali Ghasemi of Shinshu University, Japan, for providing FE-SEM micrographs.

References

[1] Nogués J, Sort J, Langlais V, Skumryev V, Suriñach S, Muñoz J S and Baró M D 2005 *Phys. Rep.* **422** 65
[2] van Lierop J, Lin K-W, Guo J-Y, Ouyang H and Southern B W 2007 *Phys. Rev.* B **75** 134409

[3] Keller J, Miltényi P, Beschoten B, Güntherodt G, Nowak U and Usadel K D 2002 *Phys. Rev.* B **66** 014431
[4] Mishra S R, Dubenko I, Griffis J, Ali N and Marasinghe K 2009 *J. Alloys Compounds* **485** 667
[5] Saha J and Victora R H 2007 *Phys. Rev.* B **76** 100405
[6] Makhlouf S A, Al-Attar H and Kodama R H 2008 *Solid State Commun.* **145** 1
[7] Salabaş E L, Rumplecker A, Kleitz F, Radu F and Schüth F 2006 *Nano Lett.* **6** 2977
[8] Punnoose A, Magnone H, Seehra M S and Bonevich J 2001 *Phys. Rev.* B **64** 174420
[9] Makhlouf S A 2004 *J. Magn. Magn. Mater.* **272–276** 1530
[10] Makhlouf S A, Parker F T and Berkowitz A E 1997 *Phys. Rev.* B **55** R14717
[11] Niebieskikwiat D and Salamon M B 2005 *Phys. Rev.* B **72** 174422
[12] Huang H X, Ding J F, Zhang G Q, Hou Y, Yao Y P and Li X G 2008 *Phys. Rev.* B **78** 224408
[13] Tang Y-K, Sun Y and Cheng Z-H 2006 *Phys. Rev.* B **73** 174419
[14] Mazumder R, Sujatha Devi P, Bhattacharya D, Choudhury P, Sen A and Raja M 2007 *Appl. Phys. Lett.* **91** 062510
[15] Park T-J, Papaefthymiou G C, Viescas A J, Moodenbaugh A R and Wong S S 2007 *Nano Lett.* **7** 766
[16] Gao F, Li P L, Weng Y Y, Dong S, Wang L F, Lv L Y, Wang K F, Liu J-M and Ren Z F 2007 *Appl. Phys. Lett.* **91** 072504
[17] Zhou S, Shi L, Zhao J, He L, Yang H and Zhang S 2007 *Phys. Rev.* B **76** 172407
[18] Koehler W C and Wollan E O 1957 *J. Phys. Chem. Solids* **2** 100
[19] For a review, Seo J W, Fullerton E E, Nolting F, Scholl A, Fompeyrine J and Locquet J-P 2008 *J. Phys.: Condens. Matter* **20** 264014
[20] Rajendran M and Bhattacharya A K 2006 *J. Euro. Ceram. Soc.* **26** 3675
[21] Li X, Cui X, Liu X, Jin M, Xiao L and Zhao M 1991 *Hyperfine Interact.* **69** 851
[22] Ita B, Murugavel P, Ponnambalam V and Raju A R 2003 *J. Chem. Sci.* **115** 519
[23] Rodriguez-Carvajal J 1993 *Physica* B **192** 55
[24] Benitez M J, Petracic O, Salabas E L, Radu F, Tüysüz H, Schüth F and Zabel H 2008 *Phys. Rev. Lett.* **101** 097206
[25] Tüysüz H, Salabaş E L, Weidenthaler C and Ferdi Schüth 2008 *J. Am. Chem. Soc.* **130** 280
[26] Salazar-Alvarez G, Sort J, Suriñach S, Baró M D and Nogués J 2007 *J. Am. Chem. Soc.* **129** 9102
[27] Berkowitz A E, Rodriguez G F, Hong J I, An K, Hyeon T, Agarwal N, Smith D J and Fullerton E E 2008 *Phys. Rev.* B **77** 024403
[28] Hernando A 1999 *J. Phys.: Condens. Matter* **11** 9455
[29] Winkler E, Zysler R D, Vasquez Mansilla M, Fiorani D, Rinaldi D, Vasilakaki M and Trohidou K N 2008 *Nanotechnology* **19** 185702
[30] Kodamaa R H, Berkowitza A E, McNiff E J Jr and Foner S 1997 *J. Appl. Phys.* **81** 5552
[31] Baltz V, Sort J, Rodmacq B, Dieny B and Landis S 2005 *Phys. Rev.* B **72** 104419
[32] Nishioka K, Hou C, Fujiwara H and Metzger R D 1996 *J. Appl. Phys.* **80** 4528
[33] Fulcomer E and Charap S H 1972 *J. Appl. Phys.* **43** 4190